

Potential biomarkers and targets in reversibility of pulmonary arterial hypertension secondary to congenital heart disease: an explorative study

Li Huang¹, Li Li², Enci Hu¹, Guo Chen¹, Xianmin Meng³, Changming Xiong¹ and Jianguo He¹

¹Center of Pulmonary Vascular Disease, State Key Laboratory of Cardiovascular Disease, Fuwai Hospital, National Center for Cardiovascular Diseases, Chinese Academy of Medical Sciences and Peking Union Medical College, Beijing, China; ²Department of Pathology, State Key Laboratory of Cardiovascular Disease, Fuwai Hospital, National Center for Cardiovascular Diseases, Chinese Academy of Medical Sciences and Peking Union Medical College, Beijing, China; ³Central Laboratory, State Key Laboratory of Cardiovascular Disease, Fuwai Hospital, National Center for Cardiovascular Diseases, Chinese Academy of Medical Sciences and Peking Union Medical College, Beijing, China

Abstract

Whether pulmonary arterial hypertension (PAH) is reversible in congenital heart disease (CHD) is important for the operability of CHD. However, little is known about that. Our research was aimed at exploring novel biomarkers and targets in the reversibility of CHD-PAH. CHD-PAH patients diagnosed with right heart catheterization (RHC) were enrolled ($n = 14$). Lung biopsy was performed during the repair surgery. After one year follow-up, mean pulmonary arterial pressures (mPAP) were evaluated by RHC to determine the diagnosis of reversible ($\text{mPAP} < 25 \text{ mmHg}$, $n = 10$) and irreversible ($\text{mPAP} \geq 25 \text{ mmHg}$, $n = 4$) PAH. Harvested normal lung tissues ($n = 6$) were included as the control group. Pulmonary arteriole lesions were identified by pathological grading in tissue staining. iTRAQ-labelled mass-spectrometry analysis followed by immunohistochemistry and western blot was used to explore the most meaningful differential proteins. For enrolled patients, the histopathological grading of pulmonary vascular lesions in reversible CHD-PAH patients was all at grades 0–II while grades III–IV were shown only in irreversible CHD-PAH patients. Proteomic analysis identified 85 upregulated and 75 downregulated proteins, including cytoskeletal proteins and collagen chains, mainly involved in cell adhesion, extracellular matrix, cytoskeleton, immune response, and complement pathways. Among them, caveolin-1, filamin A expression, and cathepsin D combined with macrophagocytes counts were significantly increased; glutathione S-transferase mu 1 (GSTM1) expression was significantly decreased in the irreversible CHD-PAH group (all $P < 0.05$). Caveolin-1, filamin A, and cathepsin D expression showed a positive relation and GSTM1 showed a negative relation with pathological grading. Upregulated caveolin-1, filamin A, and cathepsin D combined with increased macrophagocytes and downregulated GSTM1 may be potential biomarkers and targets in the irreversibility CHD-PAH, and which may be useful in evaluating the operability and understanding the irreversibility of CHD-PAH. Expression of these pathological biomarkers combined with pathological changes in lung biopsy may have great value in predicting the irreversibility of PAH.

Keywords

pulmonary arterial hypertension, congenital heart disease, reversibility, biomarkers

Date received: 17 October 2017; accepted: 5 January 2018

Pulmonary Circulation 2018; 8(2) 1–12

DOI: 10.1177/2045893218755987

Introduction

Pulmonary arterial hypertension (PAH), characterized by increased pulmonary arterial pressure (PAP), pulmonary vascular resistance (PVR), and aggravated right heart function, is a common combination of congenital heart disease (CHD) with systemic-to-pulmonary artery shunt diseases.

Corresponding author:

Jianguo He, No. 167, Beilishi Road, Xicheng District, Beijing 100037, China

Email: hejianguofw@163.com



Creative Commons Non Commercial CC-BY-NC: This article is distributed under the terms of the Creative Commons Attribution-NonCommercial 4.0 License (<http://www.creativecommons.org/licenses/by-nc/4.0/>) which permits non-commercial use, reproduction and distribution of the work without further permission provided the original work is attributed as specified on the SAGE and Open Access pages (<https://us.sagepub.com/en-us/nam/open-access-at-sage>).

© The Author(s) 2018.
Reprints and permissions:
sagepub.co.uk/journalsPermissions.nav
journals.sagepub.com/home/pul



Prevalence in studies was in the range of 4–28%,^{1,2} and 30% of unrepaired CHD patients have PAH.³ Our previous data showed an even more prevalent morbidity in our center, with 47.5% of CHD patients complicated by PAH.⁴

For unrepaired CHD, increase in pulmonary blood flow with subsequent proliferative changes in the pulmonary architecture can lead to severe increases in PVR and often result in irreversible PAH. Interventional and surgery repair as the main treatment for CHD has benefited patients. However, the operative indications and operability remain controversial. The reliability of traditional recommendations existing according to preoperative hemodynamic and vascular reaction experiment seemed limited.⁵ Some patients still got persistent PAH after the operation. Studies even showed a worse ten-year postoperative survival for patients with persistent postoperative PAH than for those with Eisenmenger syndrome (ES).^{6,7}

Because of the individual variability, the response of the pulmonary vasculature to high pulmonary blood flow is not uniform and did not occur in a predictable fashion.⁸ Current research also has not established definite and unified standards or reported any practical indicators or biomarkers in the reversibility of PAH in CHD. Why PAH should be reversible in some CHD patients but irreversible in others is still unknown. Therefore, in this study we aimed to explore novel biomarkers and targets in the reversibility of CHD-PAH through proteomics analysis to better guide treatment and understand the pathological mechanism of reversible and irreversible PAH.

Methods

Patients' inclusion and the determination of reversible and irreversible CHD-PAH

CHD-PAH patients diagnosed by RHC who met the indications of complete repair surgery were prospectively enrolled. The inclusion criteria were: (1) patients that can provide informed consent; (2) CHD-PAH patients diagnosed as congenital systemic-to-pulmonary artery shunt diseases and had not received any targeted therapy; and (3) patients who have the indication of complete repair surgery with $Q_p/Q_s > 1.5$ and $PVR < 1000 \text{ dyn/s/cm}^{-5}$. The following CHD patients were excluded: (1) those with any other PAH pathogenesis; (2) those who had repair surgery or target drugs, have mental disorders, histories of drug addiction, trisomy 21 syndrome, and other diseases that cannot provide informed consent or cooperate in the study; (3) those that have acute or chronic organic disease that cannot complete the required examinations; (4) those who are pregnant and lactating. The pulmonary arterial hypertension was defined as an increase in mean pulmonary arterial pressure (mPAP) $\geq 25 \text{ mmHg}$ at rest as assessed by RHC and pulmonary artery wedge pressure (PAWP) $\leq 15 \text{ mmHg}$ and $PVR > 240 \text{ dyn/s/cm}^{-5}$ or 3 Wood units (WU). The control patients were those that could provide normal lung tissue. Control patients with

heart disease, liver and kidney function deficiency, or other combined infectious diseases, and who could not provide informed consent were also excluded.

Patients enrolled would have RHC to confirm the PAH diagnosis. Hemodynamics and basic characteristics data were collected before the repair surgery. After the operation, patients were followed up for one year and no targeted therapy for PAH was performed during that time. One year later, patients underwent RHC to evaluate mPAP. Those with continuous PAH (mPAP $\geq 25 \text{ mmHg}$ at rest) were considered the irreversible PAH group. On the contrary, if mPAP recovered to normal, the CHD-PAH would be reversible.

This study complied with the Declaration of Helsinki and was approved by the Institutional Review Board of Fuwai Hospital.

Lung biopsy

With the patients' consent, the lung tissues of the CHD-PAH patients were obtained during the surgery and control tissues comprised regions away from tumor nidus of lobectomy specimens from patients undergoing surgery for bronchial carcinoma. Tissue sampling should also be kept away from the nidus of pulmonary atelectasis, emphysema, and fibrosis. The tissue samples were then washed with cold sterile phosphate buffered saline or normal saline several times and stored in liquid nitrogen or fixed in 4% buffered neutral formalin for further determine and analysis. Hematoxylin and eosin (H&E) and Elastica van Gieson staining were used to evaluate the pathological alteration of the lung tissues. Pathological features of the pulmonary arterioles were described according to the Heath and Edwards classification system:⁹ grade I = medial hypertrophy in arteries and arterioles without intimal alterations; grade II = medial hypertrophy with cellular intimal proliferation; grade III = medial hypertrophy, intimal fibrosis, and early generalized vascular dilatation; grade IV = progressive vascular dilatation and occlusion by intimal fibrosis and fibroelastosis; grade V = hypertrophied muscular arteries, cavernous lesions, angiomatoid lesions, and pulmonary hemosiderosis; grade VI = necrotizing arteritis.

iTRAQ labelled LC-MS/MS analysis

Fourteen harvested lung tissue specimens (four from the reversible group, four from the irreversible group, and six from the control group) were lysed in protein lysis buffer. After digestion and centrifugation, the protein supernatants were extracted and reserved. An iTRAQ reagent kit (Applied Biosystems, USA) were used for further protein precipitation, digestion, and iTRAQ-labelling. The peptide mixture was separated with HPLC system (RIGOL 3220) and analyzed by TripleTOFTM 5600 LC/MS/MS (Applied Biosystems Sciex).

Protein identification and quantification for mass spectrometry was performed with the ProteinPilot software

Beta (version 4.2, Applied Biosystems) in the Human UniProtKB/Swiss-Prot database. The first stage error was 10 ppm and the second stage error was 20 ppm. The variable modifications of phospho and phosphopantetheine were considered. To minimize false positive results, a strict cut-off for protein identification was applied with the unused ProtScore ≥ 1.5 , which corresponds to a confidence limit of 95%, and at least two peptides with the 95% confidence interval were considered for protein quantification. Proteins that have a $P < 0.05$ and identified with mass tag changes ratio ≥ 1.5 or ≤ 0.67 were reported. The data were exported with the PDST software system.

Gene Ontology (GO) functional classifications were analyzed with DAVID software (<http://david.abcc.ncifcrf.gov>). GO enrichment analysis of the differential proteins, including biological process, cellular components distribution, molecular function, and KEGG enrichment analysis, was performed to identify GO terms that were significantly enriched in differentially expressed proteins. Protein interaction network and signal pathway were analyzed with MetaCore™ software (version 6.18).

Immunohistochemical staining

The neutral formalin fixed lung tissues were made into 4–5- μ m sections after dehydration and paraffin embedding. After heating for antigen retrieval, 3% H_2O_2 was used to block endogenous peroxidase. The sections were incubated with primary antibody at 4°C overnight. All the primary antibodies were from Abcam Corporation. Primary antibody amplifier quanto and HRP polymer quanto (Ultravision Quanto Detection System HRP DAB Sample, Thermo, UK) were added for DAB coloration. After covering the slide with resin, the tissue was observed under microscope.

Western blot

The frozen tissue of each group was digested with RIPA lysis buffer to extract proteins. The BCA method was used for protein quantification. Prepared protein specimens of each group were loaded to 4–12% PAGE electrophoresis precast gels (Invitrogen). IBlot® transfer stacks that contain the required buffers and transfer membrane (nitrocellulose) were used for transfer with iBlot® 2 dry blotting device (Invitrogen). The obtained nitrocellulose membrane was blocked by TBST containing 5% non-fat dry milk at room temperature for 2 h. Nitrocellulose membrane was then incubated in the primary antibody solution at 4°C overnight. The NC membrane was washed with TBST for three times for 10 min each time. After the second wash with TBST, immunoblots were detected using a chemiluminescence kit (Thermo Scientific Pierce, Waltham, MA, USA) and the autoradiographs were quantitated via densitometry (Science Imaging System, BioRad, Hercules, CA, USA).

Statistical analysis

The gray value of the protein bands was analyzed by Quantity One. The clinical features and the gray value of the protein bands between each group was compared using independent Student's t-test. The correlation of expression of the differential proteins and pathological grading was analyzed by Spearman's correlation. All the data analyses were performed with SPSS software 23 (IBM SPSS Statistics 23, USA) and GraphPad Prism 5.0 (GraphPad, San Diego, CA, USA) programs. Statistical significance was defined as P value < 0.05 .

Results

Clinical features of the reversible and irreversible PAH patients

From April 2012 to the end of 2012, 16 CHD-PAH patients diagnosed with RHC were consecutively enrolled in this study. After repair surgery, patients were followed up for one year until the second RHC was performed. Among them, two patients were excluded for loss of follow-up. Fourteen 14 patients were eventually included; of them, 57% were women. Atrial septal defect (ASD) and ventricular septal defect (VSD) were the main etiology, accounting for 35.7% (5/14) and 57.1% (8/14), respectively. Among them, ten patients were confirmed as reversible CHD-PAH for mPAP < 25 mmHg and four patients were considered as irreversible CHD-PAH for mPAP ≥ 25 mmHg.

The clinical characteristics of the reversible and irreversible CHD-PAH patients were shown in Table 1. The mean age of reversible and irreversible CHD-PAH patients was 27.1 ± 19.7 and 46.3 ± 14.5 years, respectively ($P = 0.11$). The preoperative and postoperative mPAP were 39.5 ± 15.8 , 53.3 ± 23.4 mmHg ($P = 0.22$) and 18.9 ± 3.3 mmHg, 35.0 ± 8.8 mmHg ($P < 0.001$), respectively. The preoperative PVR was 488.4 ± 206.8 dyn/s/cm⁻⁵ and 370.1 ± 159.3 dyn/s/cm⁻⁵ ($P = 0.33$) in the reversible and irreversible groups, respectively. Three patients in the reversible group had normal pulmonary arterioles, six patients showed pathological grade I, and one patient showed grade II, while patients in the irreversible group all had abnormal pathologic changes: two in grade III; one in grade I; and one in grade II.

Six patients who met the inclusion standards and with harvested normal lung specimens were included as the control group.

Proteomic profiling of the lung tissue in reversible and irreversible PAH patients

In mass spectrometry, 85 increased expression and 75 diminished expression proteins were founded in the irreversible group compared with the reversible and control groups. Large amounts of cytoskeletal proteins and collagen chains were significantly upregulated in irreversible group, as well as macromolecules such as laminin, proteoglycan,

Table 1. The clinical features of the enrolled reversible and irreversible PAH patients.

No.	Age (years)	Gender	Etiology	Pre-sPAP (mmHg)	Pre-dPAP (mmHg)	Pre-mPAP (mmHg)	Pre-PVR (dyn/s/cm ⁻⁵)	SpO ₂ (%)	PG	Post-sPAP (mmHg)	Post-dPAP (mmHg)	Post-mPAP (mmHg)
Reversible group												
1	45	F	ASD	40	23	31	445.5	97%	I	23	11	16
2	45	F	ASD	56	37	28	312.1	97%	II	27	13	17
3	59	M	VSD	42	22	30	315.3	96%	0	26	15	18
4	5	M	VSD	47	22	27	470.6	99%	I	23	14	17
5	4	F	VSD	106	54	70	945.4	100%	I	35	8	17
6	9	F	VSD	55	23	35	284.5	98%	I	39	12	21
7	19	F	VSD	—	—	26	576.3	100%	I	39	10	23
8	13	M	VSD	88	49	62	445.4	99%	I	29	6	14
9	41	M	ASD	54	21	35	377.6	100%	0	30	12	23
10	31	F	VSD, PFO	70	40	51	710.9	92%	0	35	17	23
Irreversible group												
1	40	M	VSD	104	34	60	365.6	95%	III	63	27	35
2	65	M	ASD	63	29	40	246.5	97%	I	40	20	26
3	49	F	ASD	80	16	30	271.8	95%	III	50	25	32
4	31	F	Other	126	61	83	596.3	96%	II	70	35	47

F, female; M, male; ASD, atrial septal defect; VSD, ventricular septal defect; PFO, patent foramen ovale; SpO₂, systemic arterial oxygen saturation; other, complete endocardial cushion defect; PG, pathological grading.

and integrins. The details of the differential expressed proteins were shown in Table 2.

In bioinformatic analyses, the differential proteins participated in were involved mainly in cell adhesion (19.62%), biological adhesion (19.62%), response to wounding (15.82%), cytoskeleton organization (12.66%), actin filament-based process (10.13%), and actin cytoskeleton organization (8.86%). It indicated that the proteins were mainly related to structural molecule activity (20.89%), cytoskeletal protein binding (15.82%), and actin binding (14.56%). KEGG enrichment analysis emphasized the importance of focal adhesion, extracellular matrix (ECM)-receptor interaction, and the regulation of actin cytoskeleton. MetaCore analysis confirmed that immunoregulation, immune response signaling pathway, cellular component organization, system development, muscle contraction, positive regulation of protein metabolic process, and other pathways may be involved in the pathological process. And the complement pathways, integrin mediated cell adhesion and migration, cytoskeleton remodeling and non-junctional mechanisms mediated endothelial cell (EC) contacts were the most possible pathways that the differential proteins interacted with.

Four candidate proteins confirmed by MS analysis significantly differed between groups

According to the MS analysis, the abnormal expression of cytoskeleton proteins probably indicated an active cytoskeletal remodeling in CHD-PAH, especially in irreversible patients. Meanwhile, cell proliferation and metabolism also seemed active in irreversible patients. That led us to

pay more attention to proteins associated with cytoskeletal, cell proliferation, and metabolism in exploring the biomarkers and targets of irreversible PAH. Four proteins (caveolin-1, filamin A [FLNA], cathepsin D, and glutathione S-transferase mu1 [GSTM1]), which may be associated with PAH, were significantly differed between groups in expression. Caveolin-1, FLNA, and cathepsin D were significant increased expressions in the irreversible CHD-PAH group (1.8-fold and 4.6-fold; 2.3-fold and 4.7-fold; 3.7-fold and 4.7-fold, respectively) compared to the reversible CHD-PAH and control groups. GSTM1 expression was obviously decreased (0.033-fold and 0.023-fold) in the irreversible group than in the reversible and control groups.

Qualitative and quantitative analysis of the candidate proteins in immunohistochemical staining and western blot

To further confirm the mass spectrometry findings, immunohistochemical and western blot were used for further qualitative and quantitative analysis of the four differential proteins.

Immunohistochemical staining of the lung tissue showed that caveolin-1 was apparently expressed in pulmonary arteria smooth muscle cells (PASMC) in the irreversible group, and a little in the reversible and control groups. FLNA was positively expressed in all the groups, but was much more significant in the irreversible group. Cathepsin D was mainly expressed in macrophagocyte, the antibody-labelled macrophagocyte count seemed much higher in the irreversible group than in the reversible and control groups.

Table 2. The differential proteins in the reversible (Rev) and irreversible (Irr) CHD-PAH groups compared with the control (Con) group.

Protein name	iTRAQ-ratio Rev:Con	iTRAQ-ratio Irr:Con	iTRAQ-ratio Irr:Rev	P value Rev:Con	P value Irr:Con	P value Irr:Rev
The upregulated proteins						
Collagen alpha-I (VI) chain	0.809	3.908	4.966	0.268	0.008	0.000
Collagen alpha-I (XII) chain	0.570	2.535	4.406	0.021	0.000	0.000
Cathepsin D	1.180	4.742	3.698	0.295	0.001	0.000
Sushi domain-containing protein 2	0.731	2.805	3.597	0.509	0.001	0.000
Sodium/potassium-transporting ATPase subunit alpha-1	1.542	5.395	3.532	0.129	0.000	0.000
Basement membrane-specific heparan sulfate proteoglycan core protein	1.380	4.446	3.373	0.219	0.000	0.000
Myosin-14	1.000	3.251	3.251	0.364	0.000	0.000
Voltage-dependent-anion-selective channel protein 2	0.738	2.27	3.162	0.940	0.024	0.009
Keratin, type II cytoskeletal 7	0.581	1.888	3.133	0.048	0.014	0.000
LIM and calponin homology domains-containing protein I	0.724	2.148	2.965	0.422	0.037	0.000
Collagen alpha-6(VI) chain	1.459	4.130	2.884	0.079	0.000	0.000
Collagen alpha-2(IV) chain	1.067	2.938	2.884	0.272	0.003	0.000
Phosphoglucosyltransferase-like protein 5	1.047	2.831	2.884	0.433	0.018	0.000
Platelet glycoprotein 4	1.086	2.992	2.78	0.762	0.003	0.004
Vinculin	1.127	3.076	2.754	0.681	0.000	0.000
Matrix metalloproteinase-9	0.679	2.032	2.729	0.330	0.021	0.002
Desmin	1.770	4.742	2.704	0.278	0.000	0.000
Filamin-B	0.973	2.630	2.679	0.957	0.000	0.000
Alpha-actinin-4	1.096	2.884	2.655	0.385	0.003	0.000
Myosin-9	2.399	5.808	2.466	0.088	0.000	0.000
Transgelin	0.938	2.312	2.466	0.592	0.008	0.000
Preylcysteine oxidase I	1.66	4.093	2.466	0.010	0.000	0.000
Lactadherin	3.133	7.047	2.377	0.016	0.000	0.006
Chondroitin sulfate proteoglycan 4	1.393	3.311	2.355	0.606	0.012	0.013
Tropomyosin beta chain	1.570	3.532	2.355	0.947	0.025	0.001
Myosin light polypeptide 6	2.168	4.875	2.333	0.429	0.020	0.019
Myeloperoxidase	0.887	2.051	2.312	0.385	0.028	0.000
Filamin-A	2.032	4.656	2.291	0.015	0.000	0.000
Alpha-actinin-I	1.009	2.270	2.270	0.475	0.000	0.000
Laminin subunit beta-2	2.377	5.297	2.208	0.110	0.000	0.000
Fibulin-5	2.188	4.656	2.208	0.148	0.000	0.004
Laminin subunit alpha-5	2.148	4.487	2.188	0.064	0.000	0.000
Platelet endothelial cell adhesion molecule	2.679	5.754	2.188	0.028	0.000	0.001
Glutamyl aminopeptidase	3.945	8.551	2.168	0.030	0.000	0.001
Myosin-II	2.466	5.297	2.148	0.000	0.000	0.000
Intercellular adhesion molecule I	1.067	2.270	2.128	0.658	0.000	0.000
Tropomyosin alpha-I chain	2.249	4.699	2.109	0.305	0.000	0.000
Calreticulin	1.380	2.884	2.109	0.494	0.000	0.000
Proteasome subunit alpha type-6	0.929	2.032	2.109	0.765	0.033	0.008
Spectrin beta chain, brain I	3.133	6.486	2.089	0.000	0.000	0.000
Annexin A4	0.847	1.803	2.070	0.722	0.001	0.002
Hemiscitin-I	1.393	2.754	2.051	0.568	0.002	0.001
Cell surface glycoprotein MUC18	1.445	2.858	2.014	0.652	0.013	0.017
Integrin alpha-2	1.803	3.404	1.995	0.074	0.003	0.041

(continued)

Table 2. Continued

Protein name	iTRAQ-ratio Rev:Con	iTRAQ-ratio Irr:Con	iTRAQ-ratio Irr:Rev	P value Rev:Con	P value Irr:Con	P value Irr:Rev
Spectrin alpha chain	2.421	4.786	1.977	0.001	0.000	0.000
Myosin-10	3.076	5.916	1.923	0.010	0.000	0.000
Calnexin	2.606	4.966	1.923	0.008	0.000	0.008
Transmembrane protein 43	1.445	2.754	1.923	0.496	0.003	0.009
Acid ceramidase	1.432	2.655	1.923	0.399	0.008	0.005
Sorbin and SH3 domain-containing protein 2	1.117	2.109	1.923	0.839	0.006	0.009
Band 4.1-like protein 2	2.014	4.406	1.905	0.458	0.001	0.001
Laminin subunit gamma-2	1.368	2.559	1.888	0.321	0.000	0.000
Sulfide:quinone oxidoreductase, mitochondrial	0.964	1.854	1.888	0.791	0.002	0.001
Caldesmon	1.282	2.377	1.871	0.131	0.000	0.000
Palmitoyl-protein thioesterase 1	1.419	2.512	1.854	0.433	0.003	0.011
Caveolin-1	2.535	4.613	1.837	0.126	0.006	0.014
Membrane primary amine oxidase	1.343	2.421	1.820	0.310	0.001	0.000
Tryptase alpha/beta-1	1.837	3.281	1.803	0.729	0.001	0.002
Basal cell adhesion molecule	1.754	3.105	1.803	0.033	0.000	0.005
Laminin subunit gamma-1	1.754	3.133	1.786	0.011	0.000	0.000
Filamin-C	1.528	2.679	1.786	0.285	0.000	0.000
Erlin-2	1.380	2.399	1.786	0.640	0.009	0.023
Synemin	1.528	2.606	1.770	0.501	0.002	0.005
Fibulin-1	1.117	1.959	1.770	0.992	0.007	0.005
Cadherin-5	2.148	3.767	1.770	0.007	0.000	0.010
Early endosome antigen 1	0.912	1.644	1.754	0.687	0.001	0.000
Collagen alpha-1(XVIII) chain	1.486	2.559	1.722	0.002	0.000	0.002
Periaxin	1.754	2.992	1.690	0.166	0.000	0.000
Hexokinase-1	1.472	2.443	1.690	0.381	0.002	0.023
Myosin phosphatase Rho-interacting protein	1.159	1.923	1.690	0.534	0.015	0.039
Laminin subunit alpha-3	2.443	4.130	1.675	0.260	0.000	0.000
Myoferlin	1.107	1.786	1.660	0.779	0.003	0.001
von Willebrand factor	1.247	2.014	1.660	0.277	0.001	0.007
Integrin beta-1	2.109	3.436	1.660	0.032	0.001	0.023
Nestin	1.854	3.048	1.644	0.014	0.000	0.000
Protein disulfide-isomerase	1.528	2.466	1.629	0.568	0.001	0.002
Sorbin and SH3 domain-containing protein 1	1.138	1.837	1.629	0.561	0.004	0.004
Palladin	1.629	2.559	1.600	0.631	0.028	0.008
Nidogen-1	3.565	5.495	1.556	0.000	0.000	0.001
Integrin alpha-1	3.281	5.058	1.556	0.000	0.000	0.009
Epoxide hydrolase 1	1.690	2.582	1.556	0.003	0.000	0.013
Cytoplasmic FMR1-interacting protein 1	4.055	6.310	1.528	0.182	0.039	0.043
Glutamate dehydrogenase 1, mitochondrial	1.247	1.854	1.514	0.251	0.001	0.006
Afadin	1.159	1.738	1.514	0.930	0.007	0.006
Lysozyme C	1.786	2.655	1.500	0.745	0.034	0.047
The downregulated proteins						
Carbonic anhydrase 1	0.802	0.540	0.667	0.226	0.001	0.006
Stress-induced-phosphoprotein 1	0.731	0.497	0.655	0.267	0.001	0.007
Sorcin	0.759	0.474	0.614	0.382	0.006	0.019
Cytosolic non-specific dipeptidase	0.711	0.429	0.603	0.359	0.006	0.035
60S ribosomal protein L5	0.973	0.560	0.597	0.570	0.011	0.039
Leucine-rich alpha-2-glycoprotein	0.597	0.347	0.575	0.029	0.001	0.020

(continued)

Table 2. Continued

Protein name	iTRAQ-ratio Rev:Con	iTRAQ-ratio Irr:Con	iTRAQ-ratio Irr:Rev	P value Rev:Con	P value Irr:Con	P value Irr:Rev
Antithrombin-III	1.028	0.555	0.530	0.258	0.013	0.001
Serine/arginine-rich splicing factor 9	0.991	0.511	0.525	0.914	0.039	0.040
Ubiquitin-like modifier-activating enzyme 1	1.180	0.614	0.520	0.307	0.000	0.000
Fructose-1,6-bisphosphatase 1	1.169	0.570	0.515	0.993	0.024	0.021
Vacuolar protein sorting-associated protein 4B	0.501	0.278	0.511	0.062	0.005	0.035
Apolipoprotein B-100	1.009	0.501	0.506	0.368	0.000	0.000
Glyceraldehyde-3-phosphate dehydrogenase	0.855	0.429	0.506	0.233	0.004	0.011
Elongation factor 2	0.802	0.437	0.501	0.156	0.004	0.015
Ig gamma-2 chain C region	0.964	0.461	0.497	0.357	0.017	0.033
Ceruloplasmin	0.692	0.344	0.479	0.077	0.000	0.007
Catalase	0.904	0.461	0.466	0.387	0.012	0.006
Bifunctional purine biosynthesis protein PURH	0.920	0.413	0.457	0.290	0.002	0.009
SAM domain and HD domain-containing protein 1	1.138	0.497	0.453	0.906	0.008	0.005
Isoleucine-tRNA ligase, cytoplasmic	1.127	0.506	0.453	0.880	0.043	0.011
Plasma cell-induced resident endoplasmic reticulum protein	0.832	0.366	0.449	0.460	0.018	0.038
40S ribosomal protein S4, X isoform	0.631	0.291	0.445	0.041	0.000	0.043
Aflatoxin B1 aldehyde reductase member 2	0.759	0.319	0.425	0.076	0.002	0.021
40S ribosomal protein S13	0.780	0.319	0.413	0.469	0.015	0.016
Keratin, type I cytoskeletal 17	0.692	0.308	0.413	0.153	0.005	0.027
60S ribosomal protein L18	1.213	0.470	0.413	0.945	0.020	0.022
Plasma protease C1 inhibitor	0.863	0.350	0.409	0.289	0.000	0.000
Flavin reductase (NADPH)	0.991	0.370	0.384	0.615	0.010	0.000
Macrophage migration inhibitory factor	0.497	0.175	0.380	0.021	0.024	0.008
Histone H1.4 OS = Homo sapiens	0.895	0.322	0.366	0.693	0.013	0.044
Pyruvate kinase isozymes M1/M2	0.429	0.167	0.350	0.003	0.000	0.013
Heterogeneous nuclear ribonucleoprotein U	0.991	0.398	0.347	0.484	0.016	0.002
Alcohol dehydrogenase [NADP(+)]	0.787	0.254	0.334	0.053	0.000	0.005
60S ribosomal protein L10	0.406	0.136	0.319	0.003	0.000	0.038
Leucine-rich repeat-containing protein 59	0.780	0.251	0.313	0.412	0.014	0.036
T-complex protein 1 subunit gamma	0.879	0.268	0.308	0.232	0.001	0.004
Ig kappa chain V-IV region J1	0.938	0.288	0.305	0.749	0.033	0.042
6-phosphogluconate dehydrogenase, decarboxylating	0.938	0.296	0.296	0.609	0.002	0.010
60S ribosomal protein L4	1.117	0.337	0.294	0.555	0.021	0.001
Malate dehydrogenase, cytoplasmic	0.555	0.167	0.291	0.007	0.000	0.000
Hemopexin	0.555	0.151	0.273	0.002	0.000	0.001
Adenylate kinase isoenzyme 1	0.570	0.149	0.247	0.141	0.002	0.012
Annexin A5	0.904	0.219	0.236	0.317	0.013	0.000
Vitamin D-binding protein	0.570	0.141	0.233	0.061	0.003	0.005
Adenylate kinase 2, mitochondrial	0.991	0.229	0.231	0.078	0.000	0.005
Glutathione S-transferase P	0.649	0.153	0.229	0.744	0.038	0.017
Ig kappa chain C region	0.895	0.187	0.209	0.835	0.015	0.031
Complement C3	0.773	0.171	0.200	0.000	0.000	0.000
Apolipoprotein A-IV	0.982	0.200	0.198	0.659	0.001	0.003
Phenylalanine-tRNA ligase alpha subunit	0.773	0.157	0.189	0.057	0.005	0.011
Alpha-2-macroglobulin	0.479	0.094	0.187	0.000	0.000	0.000
Phosphatidylethanolamine-binding protein 1	0.929	0.172	0.187	0.218	0.000	0.000
Complement C4-B	0.278	0.063	0.185	0.000	0.000	0.001

(continued)

Table 2. Continued

Protein name	iTRAQ-ratio Rev:Con	iTRAQ-ratio Irr:Con	iTRAQ-ratio Irr:Rev	P value Rev:Con	P value Irr:Con	P value Irr:Rev
Alpha-2-HS-glycoprotein	0.592	0.109	0.182	0.124	0.000	0.000
Inter-alpha-trypsin inhibitor heavy chain H4	0.809	0.167	0.180	0.532	0.026	0.003
Immunoglobulin J chain	0.619	0.103	0.160	0.267	0.002	0.004
Calcyphosin	0.964	0.150	0.154	0.646	0.001	0.001
60S ribosomal protein L6	1.117	0.166	0.153	0.745	0.029	0.018
40S ribosomal protein S17-like	0.592	0.091	0.149	0.158	0.019	0.039
Apolipoprotein A-I	0.619	0.091	0.142	0.005	0.000	0.000
Alpha-I-acid glycoprotein I	0.461	0.070	0.137	0.258	0.000	0.034
Glyoxalase domain-containing protein 4	1.282	0.185	0.134	0.904	0.014	0.005
40S ribosomal protein S19	0.619	0.090	0.129	0.539	0.003	0.003
Heparin cofactor 2	0.570	0.072	0.125	0.031	0.000	0.013
Transthyretin	0.492	0.050	0.101	0.059	0.001	0.005
Polymeric immunoglobulin receptor	2.228	0.209	0.096	0.001	0.022	0.000
Hemoglobin subunit delta	1.009	0.096	0.093	0.769	0.013	0.025
Haptoglobin	0.724	0.066	0.087	0.129	0.000	0.000
60S ribosomal protein L13	0.429	0.041	0.083	0.224	0.001	0.046
Apolipoprotein A-II	0.441	0.039	0.082	0.140	0.003	0.040
Alpha-I-antitrypsin	0.592	0.054	0.080	0.003	0.000	0.000
Inter-alpha-trypsin inhibitor heavy chain H2	0.649	0.052	0.075	0.032	0.000	0.000
Ig alpha-I chain C region	1.225	0.09	0.073	0.885	0.012	0.013
Serotransferrin	0.457	0.035	0.065	0.000	0.000	0.000
Glutathione S-transferase Mu I	0.631	0.023	0.033	0.251	0.005	0.006

Staining showed that GSTM1 was mainly located at the bronchial epithelial cells and type II alveolar epithelial cells. The GSTM1 expression of the lung tissue in the irreversible group was obviously lower than in the reversible and control groups (Fig. 1).

Western blot in protein quantification of caveolin-1, FLNA, cathepsin D, and GSTM1 also supported the immunohistochemical results. Caveolin-1, FLNA, and cathepsin D expression levels in the irreversible group were significantly increased than in the other group, and the levels in the reversible group were also higher than the control group. On the contrary, the GSTM1 expression was gradually decreased from control group to irreversible group, and the differences had a remarkable statistical significance. All the *P* values were < 0.05 (Fig. 2).

Correlation analysis showed significant positive relation between pathological grading and the expression of caveolin-1 ($R = 0.784$, $P = 0.012$), FLNA ($R = 0.891$, $P = 0.001$), and cathepsin D ($R = 0.891$, $P = 0.001$), while GSTM1 was shown to be negatively related with pathological grading ($R = -0.891$, $P = 0.001$).

Discussion

In this prospective explorative study, we first systematically compared the proteomics in reversible and irreversible CHD-PAH and in normal lung tissues. Amounts of

differential proteins in different pathophysiological processes were found. We revealed first that the expression of four proteins—caveolin-1, FLNA, cathepsin D, and GSTM1—were significantly different in the irreversible CHD-PAH group in either MS analysis, immunohistochemical staining, or western blot. It indicated that those proteins may be potential biomarkers in the reversibility of CHD-PAH.

Caveolin-1

Caveolin-1, the major resident scaffolding protein constituent of caveolae, is widely distributed in epithelial, ECs, fibroblasts, and smooth muscle cells (SMC). Studies showed a decreased expression of caveolin-1 in the ECs of lung tissues from idiopathic PAH (IPAH) patients,^{10,11} while enhanced expression of caveolin-1 in pulmonary vascular SMC has been found to be pro-proliferative in IPAH.¹² Meanwhile, in animal studies, monocrotaline-induced endothelial injury disrupts EC membrane with a progressive loss of endothelial caveolin-1, but resulted in enhanced expression of caveolin-1 in SMC.¹³ Reduced caveolin-1 expression of endothelial layer and increased expression of SMC in several arteries were coupled with neointimal lesions, and neointima was present only in the arteries exhibiting enhanced caveolin-1 expression in SMC. Interestingly, intimal hyperplasia and fibrosis, neointimal plexiform lesion were closely related to the development of irreversible PAH.^{14–16}

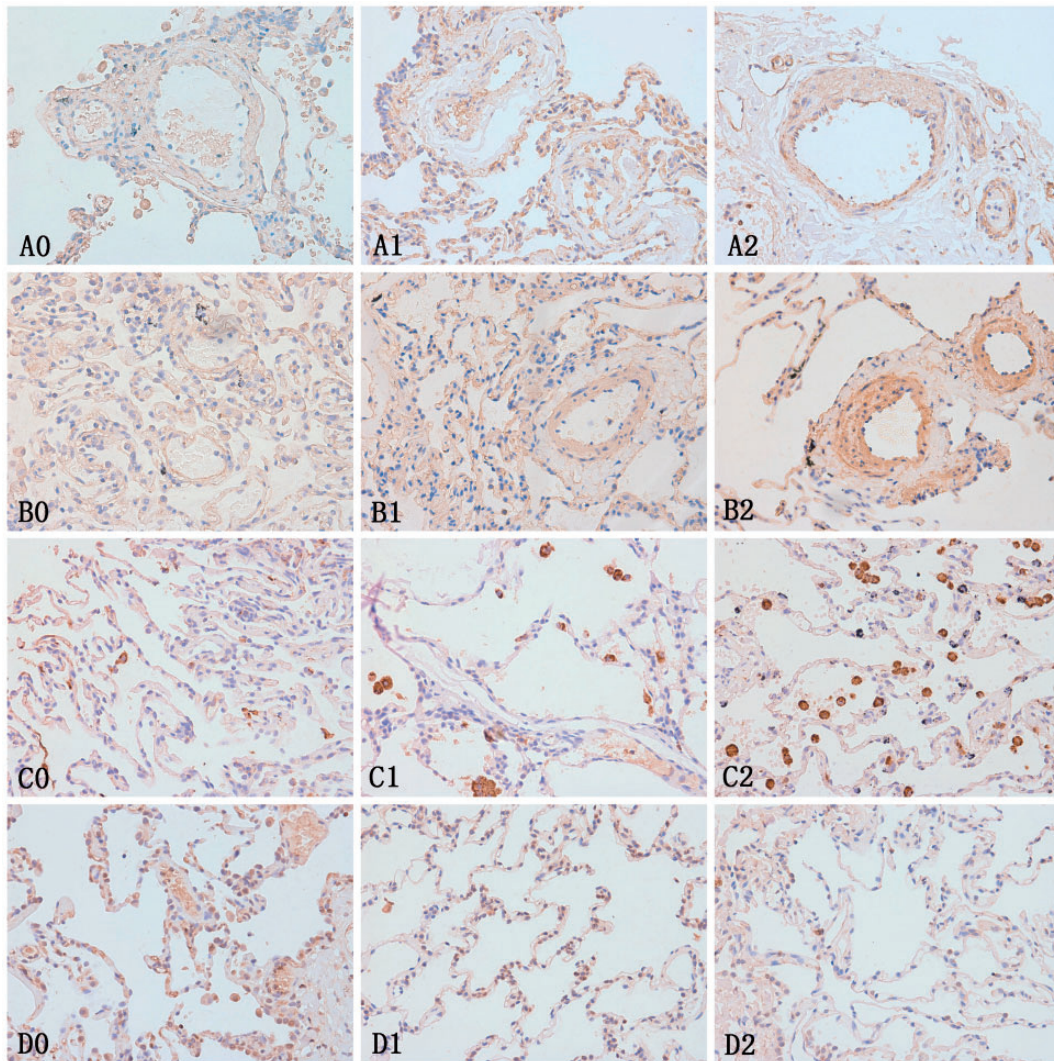


Figure 1. Immunohistochemical staining of the lung tissues for candidate proteins in each group. A0–A2: caveolin-1 expression in the lung tissue of each group, B0–B2: FLNA expression in the lung tissue of each group, C0–C2: cathepsin D expression in the lung tissue of each group, D0–D2: GSTM1 expression in the lung tissue of each group. 0, 1, 2 represent the normal, reversible CHD-PAH, and irreversible CHD-PAH groups, respectively. Caveolin-1, FLNA, and cathepsin D were significantly upregulated and GSTM1 was downregulated expression in the irreversible CHD-PAH group, compared to the reversible and control groups. These tendencies were also significant between the reversible CHD-PAH group and control group.

We may speculate that caveolin-1 is an important factor in the development of irreversible PAH. In the initial stage of CHD-PAH, abnormal hemodynamics and other factors may induce intima injury and combine with a lower expression of caveolin-1 in ECs. With the barrier effect of endothelium weakening, the medial SMCs will be exposed to the harmful stimulation directly, which may lead to an overexpression of caveolin-1 and excessive proliferation of SMCs. When the expression of caveolin-1 in SMCs reaches a certain degree, the pulmonary vascular lesion may be irreversible.

Filamin A

FLNA, a homodimer of 280 kDa, belongs to the non-muscle actin binding protein family and is widely expressed

in human tissue. The scaffolding of FLNA with cell surface receptors can regulate signaling events involved in cell shape and motility by providing mechanical stability, maintains cell–cell and cell–matrix connections, and transmits stress signals to the actin skeleton during cellular locomotion.^{17–19} A study showed that FLNA could promote tumor growth and angiogenesis.²⁰ Considering the same cancer-like characteristics of SMC as over-proliferation and anti-apoptosis in PAH, we may believe that FLNA may have the same effect as in promoting the SMC proliferation and reducing apoptosis in PAH. In this study, the high expression of FLNA in irreversible CHD-PAH pulmonary arterioles may indicate a more severe hyperproliferation in irreversible pulmonary arteriolar cells.

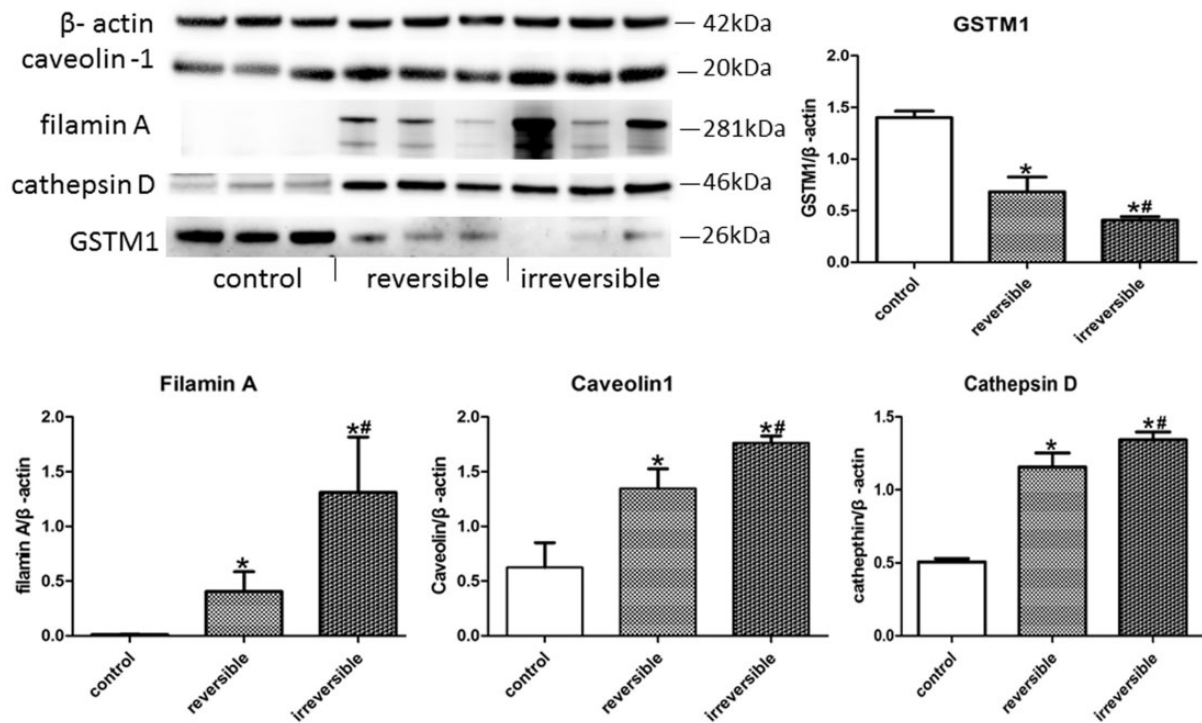


Figure 2. The expression of the four differential proteins in western blot analysis. Caveolin-1, FLNA, and cathepsin D expression levels in the irreversible group were significantly increased than in the other group, and the levels in reversible group were also higher than the control group. On the other hand, the GSTM1 expression were gradually decreased from the control group to the irreversible group, and the differences had remarkable statistical significance. *Reversible or irreversible CHD-PAH group vs. control group, $P < 0.05$. #Reversible vs. irreversible CHD-PAH group, $P < 0.05$.

Cathepsin D

Cathepsin D, a soluble aspartic protease normally resident within the acidic endosomal-lysosomal compartments, is ubiquitously present in human tissues. In the extracellular environment, enzymatically active cathepsin D can free growth factors (such as the basic fibroblast growth factor) normally embedded in the ECM to promote tumor growth and the generation of a neovascular network.^{21,22} Proteomic study had revealed an upregulation of cathepsin D and correlation to alteration in muscularization in chronic hypoxic rats, and inhibiting the increase in right ventricular systolic pressure and pulmonary arterial muscularization can significantly prevent the protein regulation under hypoxia.²³

We may think that active cathepsin D was actively released to the extracellular domain under abnormal stimuli in CHD-PAH. Cathepsin D degrades of the matrix and frees of growth factors. That all will lead to cell proliferation and angiogenesis in pulmonary arterial and then promote the development of irreversible PAH. In this study, cathepsin D expression was located mainly in macrophagocytes and may also indicate a more evident inflammatory response in irreversible PAH and may be related to the irreversibility of CHD-PAH.

GSTM1

GSTM1 belongs to the superfamily of glutathione-S-transferases, which can metabolize a broad range of reactive oxygen species (ROS) and degradation xenobiotics. Studies showed an important role of GSTM1 in tumor genesis and atherosclerosis. In an experimental model of atherosclerosis, GSTs could protect the blood vessels against oxidative stress.²⁴ Subjects with homozygous for the GSTM1 (0) allele were coming with an increased risks of hypertension and atherosclerosis.^{25,26} In in vitro experiments, knockdown of GSTM1 increased the proliferation of vascular smooth muscle cells (VSMCs) in a dose-dependent manner, as well as VSMC migration, which may suggest that GSTM1 is a novel regulator of VSMC proliferation and migration.²⁷ In our study, GSTM1 was significantly decreased in the lung tissue of irreversible CHD-PAH patients. Thus, we speculated that the decreased expression of GSTM1 may permit an environment of exaggerated oxidative stress, leading to susceptibility to PASMC proliferation and migration and vascular remodeling. That will finally contribute to the development of irreversible PAH.

In MS analysis, the obvious upregulated expression of collagen chain and basement membrane specific proteins

may indicate significant collagen deposition and matrix hyperplasia in irreversible PAH. Collagen metabolism disturbance induced collagen hyperproduction, expression, and metergasis of other related macromolecules (like laminin, integrins, cell-adhesion molecules) can lead to deposition of ECM and cell proliferation, which may ultimately thicken the blood vessel wall. In bioinformatic analyses, quite a lot of differential proteins distributed in contractile fiber and acted in cytoskeleton organization, including actin and filament-related process. The abnormal expression of cytoskeleton proteins may probably indicate an active cytoskeletal remodeling in CHD-PAH, especially in irreversible patients.

An earlier study also proposed that pulmonary vascular lesions with pathological grades I–III were potentially reversible while grades IV–VI were usually irreversible.²⁸ However, that seems unreliable. As in this study, patients with pathological change of grades I and II can also develop to persistent PAH after the operation, and all the patients with pathological grade III were showing irreversible PAH. That is to say, pathological grade III or higher may be a better predictor for irreversible PAH, but that cannot apply to pathological grades 0–II for reversible PAH.

In this study, pathological grading of pulmonary arteria in the reversible and irreversible PAH group were also well correlated with the expression of caveolin-1, FLNA, cathepsin D, and GSTM1. We can surmise that the expression changes of these four proteins can partly reflect the pulmonary arteria lesion degree. The upregulated expression of caveolin-1, FLNA, and cathepsin D and downregulated expression of GSTM1 can promote the over-proliferation and cytoskeletal remodeling of PASMC; all that may lead to the development of irreversible pulmonary arteria lesion. In our study, age, preoperative mPAP, and PVR did not differ between groups, but whether these indexes can reflect the reversibility of PAH may need to be verified by more clinical data with larger sample size.

Limitations

We also have some limitations in this study. Because of the national condition of China, many CHD patients have developed severe PAH and ES when they came to a doctor and lost the operation opportunities. Also, for many CHD patients who received the repair treatment, the increased mPAP was only due to the hemodynamic changes in the pulmonary circulation. All those patients were excluded from our study. The strict inclusion and exclusion criteria, and the difficulty in obtaining informed consent for lung biopsy and sequential RHC examination all made it difficult to enroll patients. The sample size in our study was therefore small. However, the multi-verification with pathological grading, MS, and qualitative and quantitative analysis in the same patients also made our results more credible. Meanwhile, although lung biopsy is invasive and may be unacceptable for some patients, histopathology

is important for disease diagnosis. Biomarkers in lung biopsy can be more accurate for the evaluation of reversibility in PAH than blood and clinical indicators, as it can reflect the pulmonary arteria lesion more directly. Further validation and mechanism researches will proceed in the future.

Conclusion

In this study, we preliminarily revealed that upregulated caveolin-1, FLNA, and cathepsin D combined with increased macrophagocytes and downregulated GSTM1 may be potential new biomarkers and targets in the reversibility of CHD-PAH. The expression of these pathological biomarkers combined with pathological changes in lung biopsy may have great value in predicting the irreversibility of PAH. Patients with conspicuous changes in these markers with or without obvious pathological lesion should be prudently considered before sending them to surgery, especially for those with a lower pathological grade (grades I–II). Pathological grade III or higher may present to have some value in predicting the irreversibility of PAH. We also got prima facie evidence that collagen deposition, matrix hyperplasia, cytoskeletal remodeling, and inflammation that the differential proteins contributed in may be the important pathomechanisms in the irreversible CHD-PAH development. All this will provide possible directions for exploring the reversibility of CHD-PAH. Further studies will be conducted to expound the physiopathological features and deep mechanisms of the reversibility and irreversibility of CHD-PAH.

Conflict of interest

The author(s) declare that there is no conflict of interest.

Funding

This study was supported by National Natural Science Foundation of China (Project no. 81170155) and the National Key Research and Development Program of China (project no. 2016YFC1304400).

References

1. Duffels MG, Engelfriet PM, Berger RM, et al. Pulmonary arterial hypertension in congenital heart disease: an epidemiologic perspective from a Dutch registry. *Int J Cardiol* 2007; 120(2): 198–204.
2. Engelfriet PM, Duffels MG, Möller T, et al. Pulmonary arterial hypertension in adults born with a heart septal defect: the EuroHeart Survey on adult congenital heart disease. *Heart* 2007; 93: 682–687.
3. Lindberg L, Olsson AK, Jogi P, et al. How common is severe pulmonary hypertension after pediatric cardiac surgery? *J Thorac Cardiovasc Surg* 2002; 123(6): 1155–1163.
4. Sun YJ, Pang KJ, Zeng WJ, et al. Screening study of pulmonary arterial hypertension in patients with congenital heart diseases. *Zhonghua Yi Xue Za Zhi* 2012; 92(16): 1091–1094.

5. Balzer DT, Kort HW, Day RW, et al. Inhaled nitric oxide as a preoperative test (INOP Test I): The INOP Test Study Group. *Circulation* 2002; 106: 76–81.
6. Manes A, Palazzini M, Leci E, et al. Current era survival of patients with pulmonary arterial hypertension associated with congenital heart disease: a comparison between clinical subgroups. *Eur Heart J* 2014; 35(11): 716–724.
7. Haworth SG and Hislop AA. Treatment and survival in children with pulmonary arterial hypertension: the UK Pulmonary Hypertension Service for Children 2001–2006. *Heart* 2009; 95: 312–317.
8. Walker WJ, Garcia-Gonzalez E, Hall RJ, et al. Interventricular septal defect: Analysis of 415 catheterised cases, ninety with serial hemodynamic studies. *Circulation* 1965; 31: 54–65.
9. Heath D and Edwards JE. The pathology of hypertensive pulmonary vascular disease; a description of six grades of structural changes in the pulmonary arteries with special reference to congenital cardiac septal defects. *Circulation* 1958; 18: 533–547.
10. Achcar RO, Demura Y, Rai PR, et al. Loss of caveolin and heme oxygenase expression in severe pulmonary hypertension. *Chest* 2006; 129(3): 696–705.
11. Zhao YY, Zhao YD, Mirza MK, et al. Persistent eNOS activation secondary to caveolin-1 deficiency induces pulmonary hypertension in mice and humans through PKG nitration. *J Clin Invest* 2009; 119(7): 2009–2018.
12. Patel HH, Zhang S, Murray F, et al. Increased smooth muscle cell expression of caveolin-1 and caveolae contribute to the pathophysiology of idiopathic pulmonary arterial hypertension. *FASEB J* 2007; 21: 2970–2979.
13. Huang J, Wolk JH, Gewitz MH, et al. Caveolin-1 expression during the progression of pulmonary hypertension. *Exp Biol Med (Maywood)* 2012; 237(8): 956–965.
14. Lévy M, Maurey C, Celermajer DS, et al. Impaired apoptosis of pulmonary endothelial cells is associated with intimal proliferation and irreversibility of pulmonary hypertension in congenital heart disease. *J Am Coll Cardiol* 2007; 49(7): 803–810.
15. Smadja DM, Gaussem P, Mauge L, et al. Circulating endothelial cells: a new candidate biomarker of irreversible pulmonary hypertension secondary to congenital heart disease. *Circulation* 2009; 119(3): 374–381.
16. Huang H, Zhang P, Wang Z, et al. Activation of endothelin-1 receptor signaling pathways is associated with neointima formation, neoangiogenesis and irreversible pulmonary artery hypertension in patients with congenital heart disease. *Circ J* 2011; 75(6): 1463–1471.
17. Stossel TP, Condeelis J, Cooley L, et al. Filamins as integrators of cell mechanics and signalling. *Nat Rev Mol Cell Biol* 2001; 2(2): 138–145.
18. Zhou AX, Hartwig JH and Akyürek LM. Filamins in cell signaling, transcription and organ development. *Trends Cell Biol* 2010; 20(2): 113–123.
19. Stossel TP and Hartwig JH. Filling gaps in signaling to actin cytoskeletal remodeling. *Dev Cell* 2003; 4(4): 444–445.
20. Zheng X, Zhou AX, Rouhi P, et al. Hypoxia-induced and calpain-dependent cleavage of filamin A regulates the hypoxic response. *Proc Natl Acad Sci U S A* 2014; 111(7): 2560–2565.
21. Berchem G, Glondou M, Gleizes M, et al. Cathepsin-D affects multiple tumor progression steps in vivo: proliferation, angiogenesis and apoptosis. *Oncogene* 2002; 21(38): 5951–5955.
22. Briozzo P, Badet J, Capony F, et al. MCF7 mammary cancer cells respond to bFGF and internalize it following its release from extracellular matrix: a permissive role of cathepsin D. *Exp Cell Res* 1991; 194(2): 252–259.
23. Østergaard L, Honoré B, Thorsen LB, et al. Pulmonary pressure reduction attenuates expression of proteins identified by lung proteomic profiling in pulmonary hypertensive rats. *Proteomics* 2011; 11(23): 4492–4502.
24. Misra P, Srivastava SK, Singhal SS, et al. Glutathione S-transferase 8-8 is localized in smooth muscle cells of rat aorta and is induced in an experimental model of atherosclerosis. *Toxicol Appl Pharmacol* 1995; 133(1): 27–33.
25. Eslami S and Sahebkar A. Glutathione-S-transferase M1 and T1 null genotypes are associated with hypertension risk: a systematic review and meta-analysis of 12 studies. *Curr Hypertens Rep* 2014; 16(6): 432.
26. Wang XL, Greco M, Sim AS, et al. Glutathione S-transferase mu1 deficiency, cigarette smoking and coronary artery disease. *J Cardiovasc Risk* 2002; 9: 25–31.
27. Yang Y, Parsons KK, Chi L, et al. Glutathione -S-transferase μ 1 regulates vascular smooth muscle cell proliferation, migration, and oxidative stress. *Hypertension* 2009; 54(6): 1360–1368.
28. Sakao S, Voelkel NF, Tanabe N, et al. Determinants of an elevated pulmonary arterial pressure in patients with pulmonary arterial hypertension. *Respir Res* 2015; 16: 84.